Research on Collapse Ultimate Load of Fabricated RCS Composite Frame Structure

Youquan Liu
School of Civil Engineering and Architecture, Nanchang University, Nanchang, China;
Jingang Xiong (xiongjingang@ncu.edu.cn)
School of Civil Engineering and Architecture, Nanchang University, Nanchang, China;
Jiancong Wen
School of Civil Engineering and Architecture, Nanchang University, Nanchang, China;
Moqiang Xiong
School of Civil Engineering and Architecture, Nanchang University, Nanchang, China;

Research Article

Keywords:

Posted Date: March 2nd, 2022

DOI: https://doi.org/10.21203/rs.3.rs-1407058/v1

Abstract

In this paper for study the collapse ultimate load of the prefabricated reinforced concrete column—steel beam composite frame structure, the “new RCS beam-to-column joint” is used as the beam–to-column connection to the experimental model, the half-scale fabricated RCS space frame structure (2-story, 1×2 bay) is subjected to twice instantaneous failure experiments on the bottom of side column under different load levels. The 2A column is quickly pulled out by the traction force of the vehicle. The experimental results demonstrated that the method of dismantling the failure column can relatively truly response the progressive collapse condition. The remaining RCS structure is all in the elastic stage under twice different load level tests. The displacement time history curve has no vibration phenomenon in the first experimental. The SAP2000 finite element program is used to verify that the test results are basically the same as the numerical simulation results, and it is further explored that the collapse ultimate load value is 10.25 times of the structure design load value.

Introduction

The prefabricated reinforced concrete (RC) column—steel (S) beam composite frame structure is abbreviated as the RCS composite structure, which refers to the frame structure prefabricated by precast steel beam, reinforced concrete column and composite floor slab in construction site. Compared with steel column, the concrete column of this new type composite structure has better compression resistance, greater rigidity, durability and fire resistance, saves steel, and improves the stability of the structure; Compared with reinforced concrete beam, steel beam has good flexural performance, light weight, convenient construction, reduce the component section size, and increase the effective space for use. Therefore, prefabricated RCS composite frame structure is one of the leading structural systems conforming to the development trend of building industrialization, with a broad development prospect.

Due to accidental incident, the partial failure of building structure causes chain failure of components and causes most of the structure or the whole structure to collapse, which is called progressive collapse. If the building structure collapses, it is bound to cause serious casualties and huge economic losses. In addition, the progressive collapse behavior of prefabricated RCS composite frame structure is different from that cast-in-place concrete frame structure or steel frame structure. Therefore, it is necessary to study the progressive collapse resistance performance of the prefabricated RCS composite frame structure.

Shiekh and Deierlein (1989) completed the low-cyclic repeat loading experimental on 17 joint specimens with RCS intermediate layer, studied the influence of joint failure mode, strength, stiffness and structural measures on joint performance, and the calculation formula for the joint shear strength is raised[1, 2]. Kanno and Deierlein (1993) completed low-cyclic repeat loading experimental, the capacity differences in the deformation, bearing and energy dissipation of specimens under different failure mechanisms are studied[3, 4]. Parra-Montesinos and Weight (2000) studied the seismic performance of the edge joint in the middle layer of RCS composite frame under cyclic loading[5]. Liang and Parra-Montesinos (2004) carried

out experiments on four RCS spatial joints under low cyclic loading to study the hysteretic behavior, story drift and joint deformation[6]. Chou et al. (2010) completed a series of “column through type” RCS composite frame structure (full-scale, single-story, two-bay) seismic performance experiments, verified the connection form is feasible, and studied the seismic response under different load modes[7]. Azar et al. (2013) used Open Sees for nonlinear static analysis to simulate the influence of nodes on the overall behavior of the RCS composite frame structure[8]. The results show that RCS joints can increase the lateral bearing capacity of the whole frame; Using steel beam instead of reinforced concrete beam, the overall performance has been greatly improved.

In 1968, the collapse of the Ronan Point apartment in the United Kingdom for the first time caused the architecture to pay close attention to the progressive collapse. In 1970, the United Kingdom included the progressive collapse resistance to the building code. In 1975, Canada added a clause to prevent structural collapse in building code. Other countries, including Sweden, Denmark and the Netherlands, have also added the progressive collapse provisions for the code. Then Japan (2005) and other countries also compiled the specification of progressive collapse of structural[9]. Progressive collapses to catch the attention of Americans after the events of the Murrah Federal Building and the World Trade Center (2005) [10–13]. Although these regulations emphasize the importance and harm of progressive collapse to the structure, some regulations are not specific enough and vague in meaning, which is inconvenient for practical operation.

In this paper, the “new RCS beam-to-column joint” (2020)[14] is applied to the beam-to-column connection, and a half-scale prefabricated RCS space frame structure (1×2-bay, 2-story) is manufactured as the experimental model. For to explored the collapse ultimate load, the experimental model is subjected to twice column instantaneous failure under different load levels. The weakened column (2A) is rapidly pulled out by the traction force of the vehicle, and the displacement and strain at the important position are recorded by the dynamic data acquisition instrument. Method of the failure column demolition in this paper is safer and easier to operate than the hydrogen gas-gun impact is raised by the University of Southern California, the hydrogen gas-gun impact method can be found in the paper by Kunnath et al. (2015)[15].

This paper verifies that the collapse ultimate load value of the fabricated RCS composite frame structure is 10.25 times of the structure design load value. The experimental results also reveal the dismantle method of the failure column is safe and feasible.

Experimental Program

Model selection. The “new RCS beam-to-column joint” (2020)[14] developed by our research group is applied to the beam-to-column connection of the prototype structure, and the prototype structure designed with the requirements of Chinese building Codes (2010)[16-18]. The experimental model is taken from A to B span and 1 to 2-story of the prototype structure, and it is scaled down to 1/2.

“New RCS beam-to-column joint” model. The “new RCS beam-to-column joint” (2020)[14] includes joint steel hoop, cross web, level stiffener, and cantilever beam section. The specification of joint steel hoop is 350 mm×350 mm×500 mm×12 mm, the cross web and horizontal stiffeners are welded inside it, and the cantilever beam of length 2000 mm is welded outside it. The “new RCS beam-to-column joint” (2020)[14] specifications shown in Table 1, the constructional and connection are shown in Fig. 1 and Fig. 2.

Table 1 specifications of “new RCS beam-to-column connection”

Name	Size (mm)	Height/Thickness/Length (mm)
Joint steel hoop	350×350×12	Height:500
Cross web	500×326	Thickness:10
Level stiffener	20×70	Thickness:9
Cantilever beam section	300×150×6.5×9	Length:200
Steel plate A	315×150	Thickness:8
Steel plate B	315×70	Thickness:8
Steel plate C	355×240	Thickness:8

Experimental prototype. In this paper, the prefabricated RCS structure prototype (3×4-bay, 5-story) is designed with the requirements of Chinese Building Codes (2010)[16-18]. The C40 (HRB335, Q345) is used for concrete (rebar, steel member). The cross-section size of the steel beam (concrete column, open trough steel sheeting composite floor) is 600 mm×300 mm×13 mm×18 mm (700 mm×700 mm, 80 mm). The seismic design intensity of the structure prototype is 7-degree, whose peak ground acceleration (PGA) corresponding to the exceeding probability of 10% in 50 years is 0.1 g, in which g is the acceleration of gravity. The perspective view and plan view are shown in Fig. 3 and Fig. 4.

Experimental model. The experimental model is taken from (A to B span) and (1 to 2-story) of the prototype structure, and it is scaled down to 1/2. The membrane effect of the slab is not considered in experimental model, the cross-section size of the steel beam (concrete column) is 300 mm×150 mm×6.5 mm×9 mm (350 mm×350 mm), experimental model is 3 meters spans in both the X and Y directions, the first (second) storey of the experimental model is 2 m (1.8 m) in height, and the foundation is replaced by ground beam. The same batch of concrete material characteristic are tested, the mean compressive-strength (f_{cu}) are 39 MPa. The experimental model is shown in Fig. 5, and the photo of the scene reinforcement, the reinforcement of column and foundation are shown in Fig. 6 - Fig. 8.

Experimental Scheme

For to explore the collapse ultimate load of the prefabricated RCS structure, the test model is carried out twice instantaneous failure experiments under different load levels. The failure column is constrained vertically after the remaining RCS structure is stationary (first experimental), and then increase the load for second experimental.

Loading scheme. The first experimental load is the 2.5 layers design load from the most influential area of the prototype structure. After the first experimental, it is found that the remain RCS structural are less deformation, and whose is in the early elastic stage, the 2.5 layers design load is far less than the collapse ultimate load value. For to explore the collapse ultimate load, the load is increased at the basis of the first experimental, and the second experimental load is the 5 layers design load in the most affected area of the prototype structure. Due to the limited loading space of the experimental model, the load cannot be added to continue the experimental after the second experimental. However, for to explore the collapse ultimate load value, the SAP2000 finite element program is used for simulation analysis in this paper.

In the first experimental, the amount of load is 68.4 kN. After the remaining RCS structure is stationary, steel columns and several pieces of thin steel plates are used to constrain the failure columns vertically. The first experimental load is shown in Fig. 9. The amount of load is 140.4 kN in the second experimental, and the second experimental load is shown in Fig. 10.

Failure column removed scheme. In the first experimental, the weaken part of the failure column includes steel column, steel roll bar, embedded steel plate from bottom to top, the photo of failure column is shown in Fig. 11(a). Two steel columns and several pieces of thin steel plates are used to constrain the failure column vertically after the remaining RCS structure is stationary.

In the second experimental, the weaken part of the failure column includes sheet steel, steel column, and embedded steel plate from top to down, the photo of failure column is shown in Fig. 11 (b). Accidental impact event is one of the conditions that cause progressive collapses. For to get closer to the accidental crash events, the weaken part of failure column is pulled out quickly by the vehicle traction force. The wirerope is respectively fixed on the reserved rings, the opposite end is attached to the car tow hook. The method of demolition the failed column for the second experimental is the same as that for the first experimental.

Date test scheme. For to meet the requirements of data acquisition, the dynamic data acquisition instrument is used to record. The displacement sensors are set at the Z direction of the column 2A top and the X (Y) direction of column 1A (2B). Four beam-to-column joints are selected as Joint1-Joint4. Upper flange steel plate A, web steel plate C, lower flange steel plate A and B are set as strain measurement points in each Joint, and they are respectively named as [illegible]. Displacement and strain test points are shown in Fig. 12, Strain distribution is shown in Fig. 13.

Experimental Results

First experimental results and analysis. As can be seen from Fig. 14(a), (b) and (c), the vertical displacement of top of failure column (2A) rapidly reach 1.52 mm within 0.26 s when weaken part is pulled out, and then the displacement quickly becomes stable at 1.64 mm. The displacement of column A1 rapidly reached 0.67 mm within 0.46 s, and rebounded slightly between 0.46 s and 1.94 s, and then the displacement tends to be stable at 0.67 mm. The displacement of column B2 in the Y direction rapidly reaches 1.28 mm within 0.40 s, and then the displacement tends to be stable at 1.3 mm. Compared with the cast-in-place concrete structure, the prefabricated RCS composite frame structure has no vibration phenomenon when the load is small. The author believes that the vibration needs to overcome the work done by bolt slippage and consume vibration energy, so the time history curve of displacement dose not fluctuation up and down.

The remaining RCS structure does not enter the stable state immediately after rapidly reaching the instantaneous maximum displacement, but enter the slow development state. When the remaining RCS structure is stable, two steel columns and several sheet steels are used to constrain the vertical direction of the A2 column.

As can be seen from Fig. 15(a) and (b), the time history curve of strain and displacement are basically the same and both reach the maximum immediately. The tensile strain rapidly reached 29.98 με at Jiont 1-□, and then recovered to 26.2 με and become stable. The compressive strain quickly reached -31.9 με at Jiont 1-□, and then recovered to -28.6 με and become stable. In the first experimental, the change of the other 14 strains is small, which is not expressed in this paper.

Second experimental results and analysis. The column 2A top displacement in Z direction is shown in Fig. 16(a). Because the screw diameter is 2 mm smaller than bolt hole diameter, the Z direction displacement reaches 2.255 mm immediately during the period from 0 s to 0.02 s. The contact time is 0.02 s to 0.533 s between the bolt and the inner wall of the hole. The displacement in Z direction increases more slowly than that in the previous 0.02 s. The Z direction vibration appears in 0.53 s to 4.2 s, and it entered a stable development stage after 4.16 s.

The column 2B displacement in Y direction is shown in Fig. 16(b). The initial response of the column 2A is ahead of column 2B about 0.146 s. It rapidly increases to 2.49 mm within 0.67 s, and the Y direction swings between 0.68 s to 1.26 s, with the swing peak is 2.60 mm. The swing duration of column 2A in the Z direction is longer than column 2B in the Y direction. The author thinks that when the vibration is transmitted to the 2B column joint, it needs to overcome the work done by bolt slippage and consumes the vibration energy.

Displacement of the column 1A is shown in Fig. 16(c). It rapidly increases to 1.012 mm from 0 s to 0.683 s, and then swings between 0.678 s to 1.069 s, and finally enter a stable growth stage after 1.071 s.

Time history curves of strain in second experimental are shown in Fig. 17. The maximum compressive strain at Jiont 2-□ is 94.22 με and tends to 83 με after stabilization. The maximum pull strain at Jiont 2-□ is 103.09 με and tends to 89.53 με after stabilization. The maximum pull strain at Jiont 2-□ is 122.9 με

and tends to 109.13 με after stabilization. Join 1-□ test point is pulled, and Join 1-□ and Join 1-□ test points are compressed, the maximum compressive strain at Jiont 1-□ is 110.84 με and tends to 102.6 με after stabilization. Join 3-□ test point is compressed, and Join 3-□ and Join 3-□ test points are pulled. Join 4-□ test point is pulled, and Join 4-□ and Join 4-□ test points are compressed. The strain of Jiont 1 (2) (3) and (4) are far less than the yield strain and all of them are in the early elastic stage, the remaining RCS structure is also in the elastic stage.

The shear strains at Jiont 1-□, Jiont 2-□, Jiont 3-□ and Jiont 4-□ do not change during the test. According to the study, the steel plate C cannot be transferred by shear force when the axial force of column 2A is transferred to the beam-to-column joint, but by the friction force of bolts on the web.

Numerical analysis

First experimental numerical analysis. The SAP2000 finite element models is shown in Fig. 18. In the failure condition of A2 column, the time history curve of displacement is shown in Fig. 19(a), (b) and (c). By to compare the experimental value with the finite-element value, it can be seen that the former displacement has no fluctuation section, while the latter displacement has fluctuation section, but the overall displacement variation trend of both is basically the same.

Second experimental numerical analysis. Under the same failure condition of column A2, the time history curves of displacement are shown in Fig. 20. At the moment of failure, the displacement of joint 10 (8, 11) in X (Y, Z) direction increases quickly and reaches a peak, and then do attenuation vibration until dynamic force is zero and the vibration stops. Because the E will add to a certain degree under high speed, so that the finite-element value is slightly larger than the experimental value, but the general trend is basically the same, which E is elasticity modulus.

Numerical analysis of collapse ultimate load. According to the U.S. Public Affairs Bureau GSA2003, the SAP2000 finite element program is used to further explore the collapse ultimate load value. The collapse resistance of RCS structure is evaluated by comparing the collapse ultimate load value with the design load value. When the line load increases to 334 kN /m on the steel beam, the plastic rotation angle of the horizontal steel beam is 12.76° (the maximum displacement is 489.4 mm), which exceeds the limit specified in GSA2003, and the experimental model will progressive collapse. The line load is converted into 1500 kN in the most influential area, which is 10.25 times the design load value and far larger than the design load value of the structure. Therefore, it can be seen that the RCS structure designed with China's building codes (2010)[16-18] is relatively conservative.

Conclusions

In this paper, aiming to explore the collapse ultimate load of the prefabricated RCS composite frame structure, the “new RCS beam-to-column joint” (2020)[14] is applied to the experimental model. In addition, the complete set of method for demolition the column 2A is proposed, and the half-scale experimental

model (2-story, 1×2 bay) is made, and the progressive collapse resistance is studied by the experimental and the numerical analysis. The following conclusions can be drawn:

- For the progressive collapse resistance experimental of large space frame structure, the weakened column (2A) is rapidly pulled out by the traction force of the vehicle, the method is simple to install, safe, high operability, and little interference for high-speed data acquisition, and the experimental results show that the method can relatively truly response the progressive collapse condition.
- After the first experimental, the steel beams connected to the column 2A are all in the beam mechanism stage, while the remaining RCS structure are in the initial elastic stage. After the second experimental, the remaining RCS structure is still in the elastic stage.
- When the load value is 68.4 kN, the displacement time history curve of RCS structure is different from that of cast-in-place concrete structure. Specifically, the cast-in-place concrete structure has displacement vibration phenomenon, while the RCS structure has no displacement vibration phenomenon. When the displacement suddenly reaches the maximum, the restoring force needs to overcome the bolt slip to do work, and the vibration is offset by friction energy consumption.
- Numerical analysis results agree well with the experimental ones, which verifies numerical analysis is valid. SAP2000 is used to further to explore the collapse ultimate load of the prefabricated RCS structure, which is 10.25 times of the design load. The results show that the prefabricated RCS composite frame structure designed by the Chinese building codes (2010)[16–18] has sufficient performance on the progressive collapse resistance after demolition the single side column.

Declarations

Acknowledgement

The authors gratefully acknowledge the financial support provided by the National Natural Science Foundation of China (51768044, 52068051).

Author contributions

JG X initiated the research, YQ L wrote the main manuscript, including the text, figures and tables, JG X and YQ L conducted the experiment work, JC W and MQ X assisted in the construction for the experimental model.

Data availability statement

The datasets used and/or analyzed during the current study are available from the corresponding author on reasonable request. All data generated during this study are included in this published article.

Competing interests

The authors declare no competing interests.

Additional information

Correspondence and requests for materials should be addressed to Jingang Xiong.

References

1. Sheikh TM, Deierlein GG, Yura JA, Jirsa JO (1989) Beam-column moment connections for Composite Frames: Part 1. Journal of Structural Engineering 115:2858–2876. DOI: 10.1061/(asce)0733-9445(1989)115:11(2858)
2. Deierlein GG, Sheikh TM, Yura JA, Jirsa JO (1989) Beam-column moment connections for Composite Frames: Part 2. Journal of Structural Engineering 115:2877–2896. DOI: 10.1061/(asce)0733-9445(1989)115:11(2877)
3. Kanno R, Deierlein GG. (1993) Strength, deformation, seismic resistance of joints between steel beams and reinforced concrete columns.
4. Kanno R□Deierlein GG. (1996) Seismic behavior of composite(RCS) beam-column joint subassemblies[J]□Composite Construction in Steel and Concrete □□Proceedings of an Engineering Foundation Conference.
5. Parra-Montesinos G, Wight JK (2000) Seismic response of Exterior RC column-to-steel beam connections. Journal of Structural Engineering 126:1113–1121. DOI: 10.1061/(asce)0733-9445(2000)126:10(1113)
6. Liang X, Parra-Montesinos GJ (2004) Seismic behavior of reinforced concrete column-steel beam subassemblies and frame systems. Journal of Structural Engineering 130:310–319. DOI: 10.1061/(asce)0733-9445(2004)130:2(310)
7. Chou CC, Chen JH, Chen YC, Tsai KC (2006) Evaluating performance of post-tensioned steel connections with strands and reduced flange plates. Earthquake Engineering & Structural Dynamics 35:1167–1185. DOI: 10.1002/eqe.579
8. Azar BF, Ghaffarzadeh H, Talebian N (2013) Seismic performance of composite RCS Special Moment Frames. KSCE Journal of Civil Engineering 17:450–457. DOI: 10.1007/s12205-013-1431-5
9. Japanese Society of Steel Construction Council on Tall Buildings and Urban Habitat. Guidelines for Collapse Control Design[S]. 2005.
10. Hayes JR, Woodson SC, Pekelnicky RG, Poland CD, Corley WG, Sozen M (2005) Can strengthening for earthquake improve blast and progressive collapse resistance? Journal of Structural Engineering 131:1157–1177. DOI: 10.1061/(asce)0733-9445(2005)131:8(1157)
11. Sasani M, Bazan M, Sagiroglu S (2007) Experimental and analytical progressive collapse evaluation of actual reinforced concrete structure. ACI Structural Journal. DOI: 10.14359/18955
12. Seffen KA (2008) Progressive collapse of the World Trade Center: Simple Analysis. Journal of Engineering Mechanics 134:125–132. DOI: 10.1061/(asce)0733-9399(2008)134:2(125)

13. Bao Y, Kunnath SK, El-Tawil S, Lew HS (2008) Macromodel-based simulation of progressive collapse: RC Frame Structures. Journal of Structural Engineering 134:1079–1091. DOI: 10.1061/(asce)0733-9445(2008)134:7(1079)
14. Li ZC, Xiong JG (2020) A connection mechanism of beam - column joints in RCS composite structure. CN210713245U. (in Chinese).
15. Xiao Y, Kunnath S, Li F, Zhao Y, Lew H, Bao Y (2015) Collapse test of three-story half-scale reinforced concrete frame building. ACI Structural Journal. DOI: 10.14359/51687746
16. Ministry of Housing and Urban-Rural Development of the People's Republic of China (MOHURD). Code for design of concrete structures. (GB50010-2010). Beijing; 2010. (in Chinese).
17. Ministry of Housing and Urban-Rural Development of the People's Republic of China (MOHURD). Code for seismic design of buildings. (GB50011-2010). Beijing; 2010. (in Chinese).
18. Ministry of Construction of the People's Republic of China (MOHURD). Code for design of steel structures. (GB50017-2017). Beijing; 2013. (in Chinese).
19. Mh A, Jya B, Bho C, et al. Progressive collapse resistance of post-tensioned concrete beam-column assemblies under a middle column removal scenario[J]. Journal of Building Engineering, 2020, 34.
20. Kl A, Zc A, Yi L B, et al. Uncertainty analysis on progressive collapse of RC frame structures under dynamic column removal scenarios. 2021.
21. Lian M, Cheng QQ, Su MZ, Guan BL, Zhang H (2021) Seismic performance of high-strength steel framed-tube structures with web-bolted double-channel shear links. The Structural Design of Tall and Special Buildings. DOI: 10.1002/tal.1888
22. Liu Y, Xiong J, Wen J (2021) Experimental study on the progressive collapse resistance of two-storey half-scale fabricated reinforced concrete column-steel beam composite frame structure. Advances in Civil Engineering 2021:1–14. DOI: 10.1155/2021/6603492

Figures

Figure 1

Constructional detail of “new RCS beam-to-column connection”

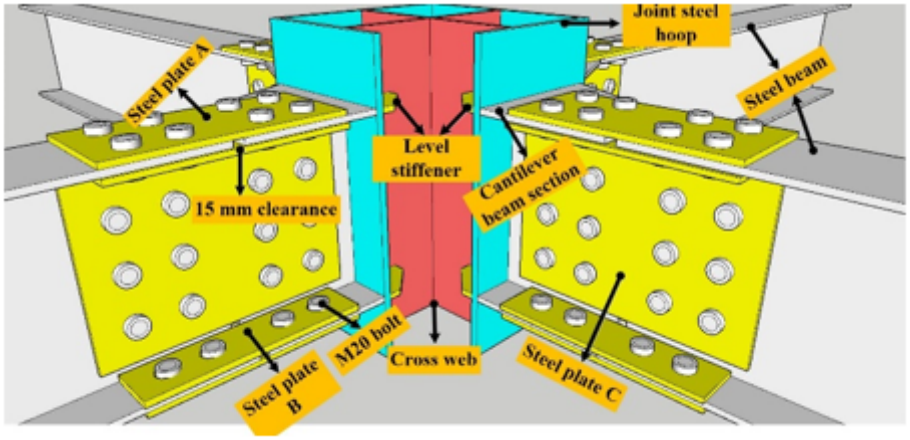

Figure 2

Connection diagram of “new RCS beam-to-column connection”

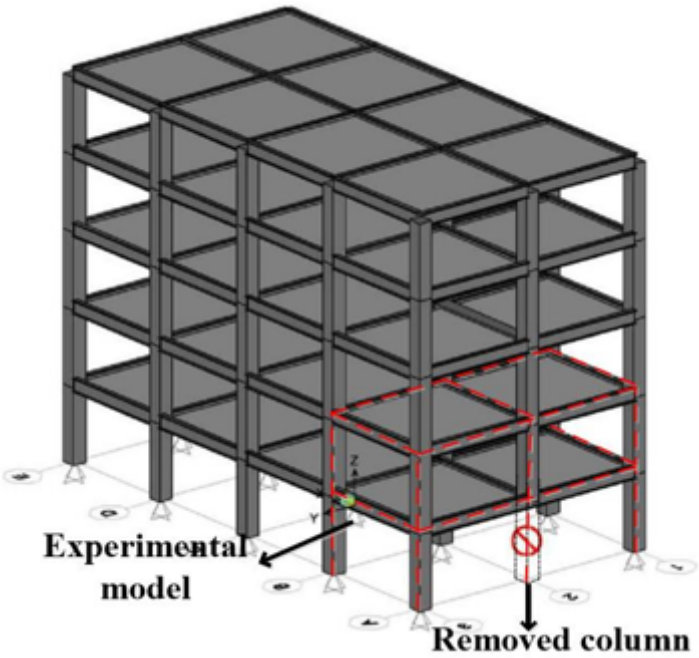

Figure 3

Perspective view

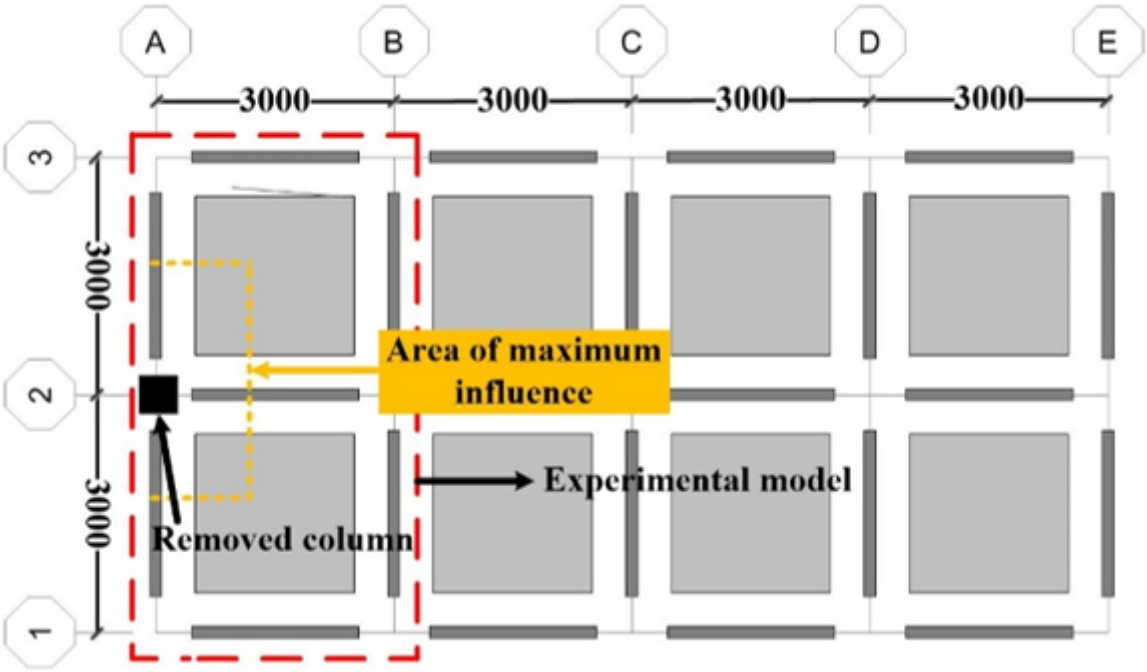

Figure 4

Plan view

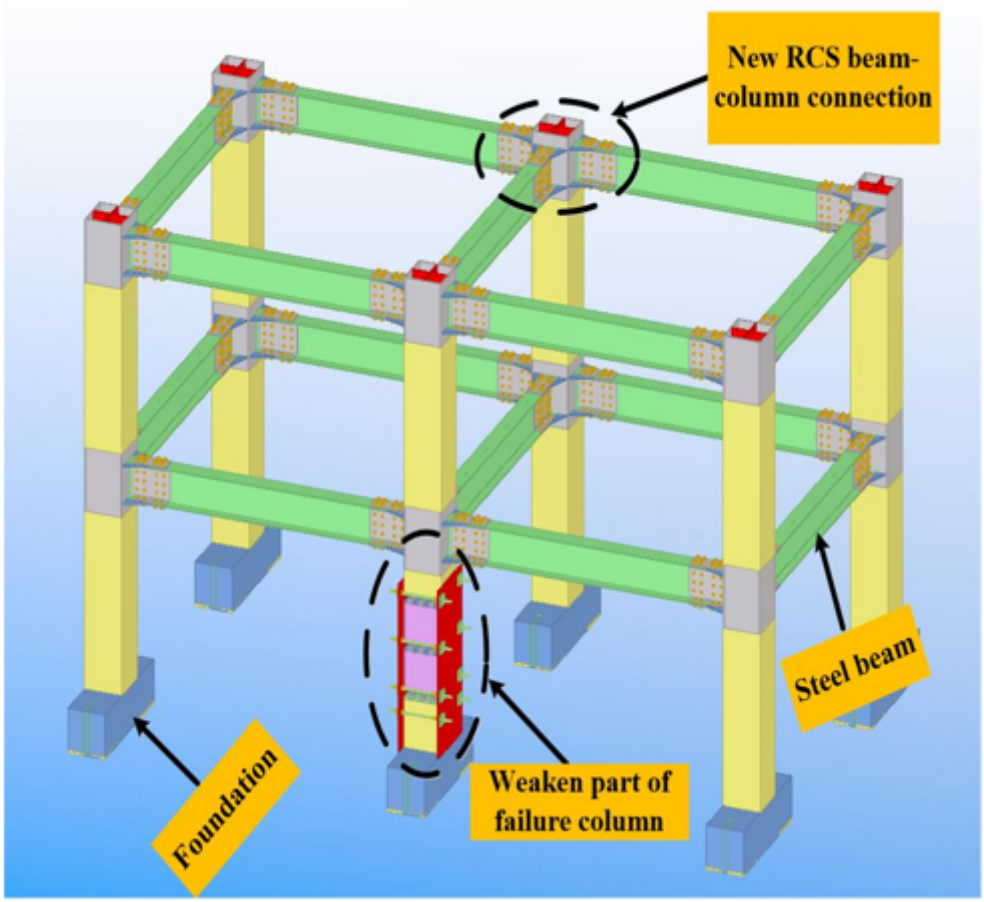

Figure 5

Experimental model

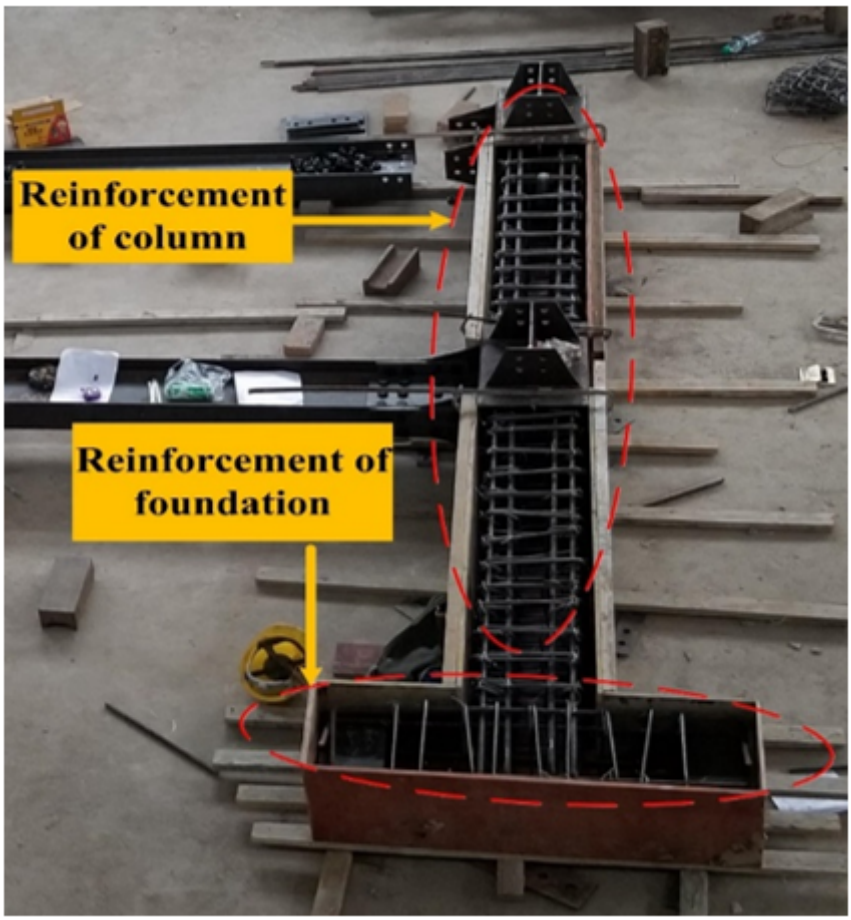

Figure 6

Photo of the scene reinforcement

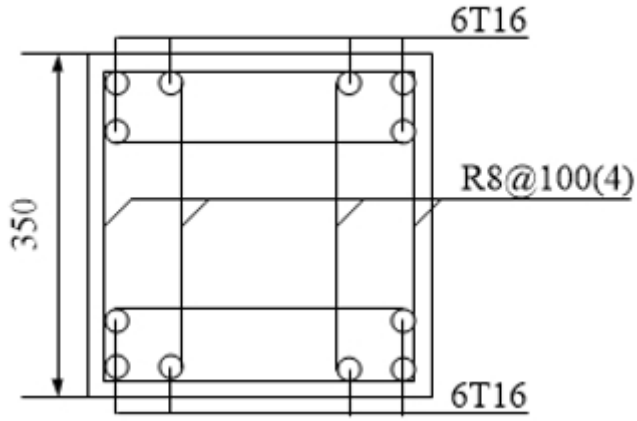

Figure 7

Column reinforcement

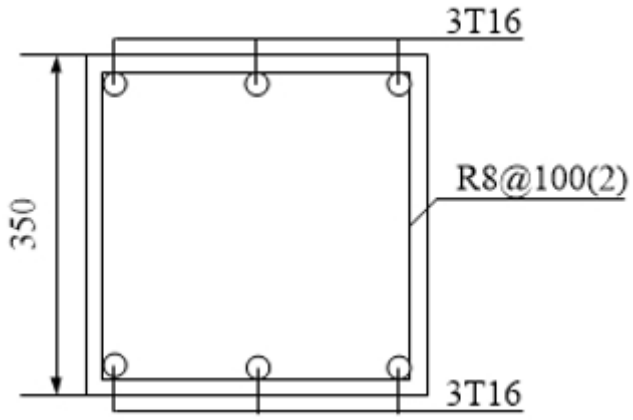

Figure 8

Foundation reinforcement

Figure 9

First experimental load

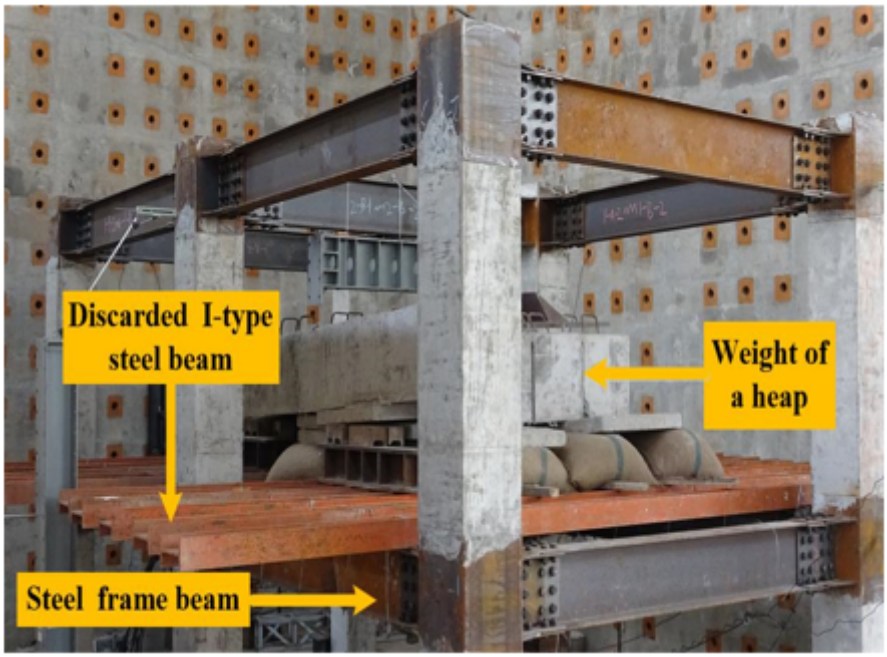

Figure 10

Second experimental load

Figure 11

Photos of failure column

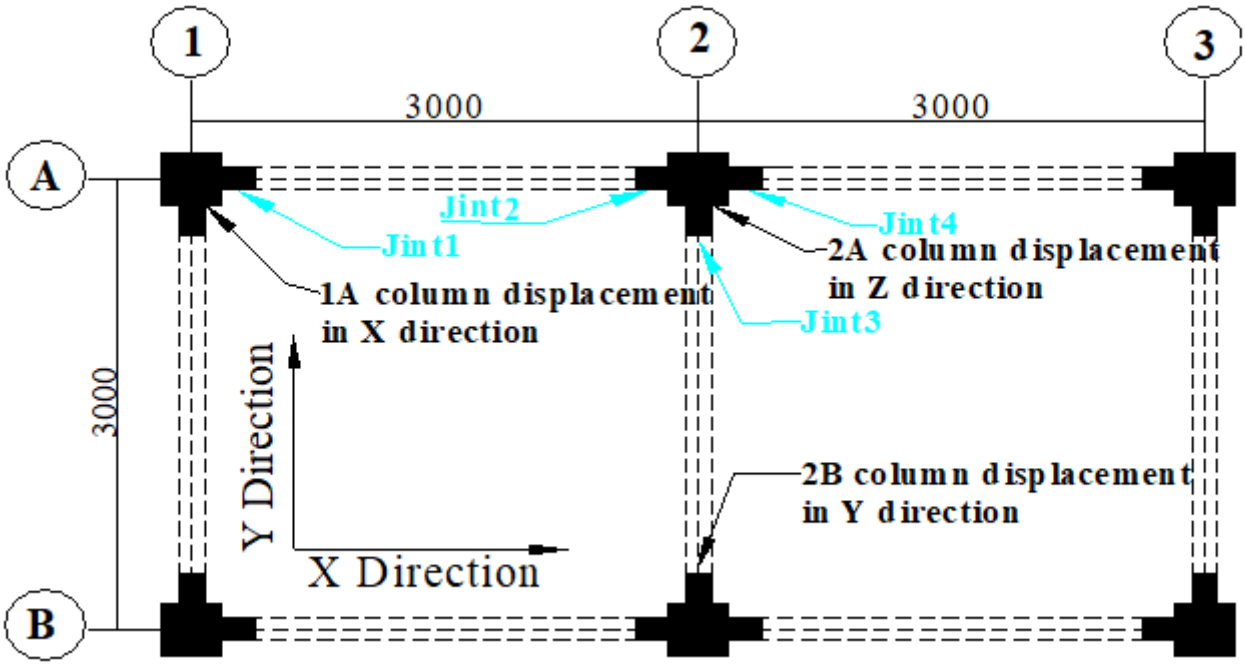

Figure 12

Displacement and strain test points

Figure 13

Strain distribution

Figure 14

Time history curves of displacement in first experimental

Figure 15

Time history curves of strain in first experimental

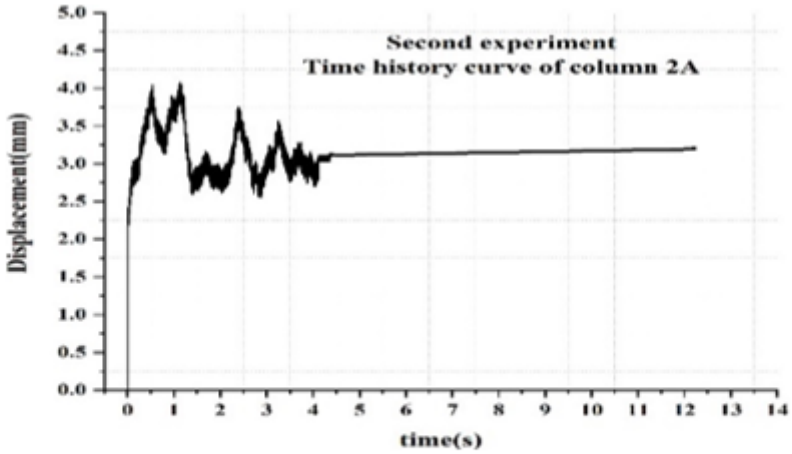

(a) Column 2A top displacement in Z direction

Figure 16

Time history curves of displacement in second experimental

Figure 17

Time history curves of strain in second experimental

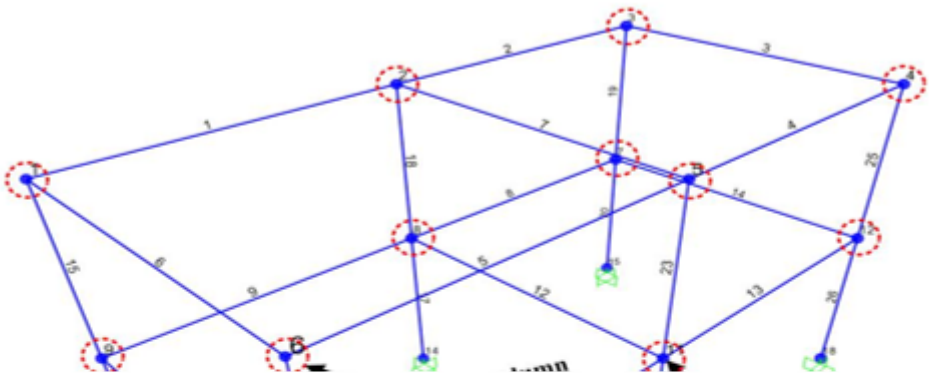

Figure 18

Finite element model

Figure 19

Time history curves of displacement in first experimental

Figure 20

Time history curves of displacement in second experimental

Supplementary Files

This is a list of supplementary files associated with this preprint. Click to download.

- Highlights.docx